

**Biomedical Signal Processing (Q)**  
**Final Report on ECG Filtering Using the IIR Method**



Written by:

Muhammad Farid Alfaruq (5023231008)

Lecturer:

Nada Fitriyatul Hikmah, S.T., M.T.

**BIOMEDICAL ENGINEERING DEPARTMENT**  
**FACULTY OF INTELLIGENT ELECTRICAL AND INFORMATICS**  
**TECHNOLOGY**

**2025**

# CHAPTER I

## THEORITICAL BACKGROUND

### 1. ECG Characteristics

The electrocardiogram (ECG) is a non-invasive diagnostic tool that records the electrical activity of the heart over time. A typical ECG waveform comprises several components: the P wave, QRS complex, and T wave, each representing specific phases of cardiac electrical activity. The standard bandwidth for diagnostic ECG signals ranges from 0.05 to 100 Hz, with a recommended sampling rate of 500 Hz.

The PhysioNet Apnea-ECG Database provides 70 single-lead ECG recordings, each ranging from approximately 7 to 10 hours in duration, sampled at 100 Hz. These recordings are annotated on a per-minute basis to indicate the presence or absence of sleep apnea events, offering valuable data for the study of sleep-related breathing disorders. Similarly, the MIT-BIH Arrhythmia Database comprises 48 half-hour excerpts of two-channel ambulatory ECG recordings, sampled at 360 Hz. These recordings include detailed annotations of over 110,000 heartbeats, categorized by type, and have been instrumental in the development and evaluation of arrhythmia detection algorithms.

### 2. ECG Noise

ECG signals are often affected by various types of noise and artifacts that can obscure the true cardiac waveform and lead to misinterpretation. Common sources of interference include low-frequency disturbances from respiration, patient movement, or poor electrode contact; narrowband electromagnetic interference typically originating from power lines; and high-frequency disruptions caused by muscle activity or fluctuations in electrode-skin impedance. These artifacts can distort the ECG signal significantly, reducing the reliability of cardiac assessments and necessitating effective filtering or preprocessing techniques to ensure accurate analysis.

To facilitate the study of noise effects, the MIT-BIH Noise Stress Test Database was developed by adding calibrated amounts of noise to clean ECG recordings from the MIT-BIH Arrhythmia Database. This auxiliary database includes recordings contaminated with common noise types like baseline wander, muscle artifacts, and electrode motion artifacts, providing a valuable resource for testing and validating ECG denoising algorithms.

Similarly, the PhysioBank Apnea-ECG Database contains 70 ECG recordings, each approximately 8 hours long, aimed at studying sleep apnea. These recordings include annotations indicating the presence or absence of apnea events, derived from simultaneously recorded respiration signals.

While the database does not explicitly annotate noise types, the long-duration recordings inherently encompass various noise artifacts typical in overnight ECG monitoring, such as baseline wander due to respiration, power-line interference, and motion artifacts. Researchers utilizing this database often need to implement preprocessing steps to mitigate these noise components before analyzing the ECG signals for apnea detection.

### **3. Digital Filter**

IIR filters can achieve sharp frequency responses with lower filter orders compared to FIR filters, making them computationally efficient. However, they may introduce phase distortion and require careful design to ensure stability. Low-pass filters allow signals with frequencies below a certain cutoff frequency to pass through while attenuating higher frequencies. High-pass filters, conversely, permit signals with frequencies above a specified cutoff to pass, attenuating lower frequencies. Band-pass filters combine these characteristics, allowing signals within a specific frequency range to pass while attenuating frequencies outside this range. These filters can be implemented by cascading low-pass and high-pass filters, effectively creating a band-pass response. The design of such filters involves selecting appropriate filter orders and cutoff frequencies to meet the desired specifications.

### **4. IIR Fundamentals**

Infinite Impulse Response (IIR) filters are characterized by their feedback mechanism, where the output depends not only on current and past input values but also on past output values. This feedback allows IIR filters to achieve a desired frequency response with fewer coefficients compared to FIR filters, making them computationally efficient. Common types of IIR filters include Butterworth, Chebyshev, and Elliptic filters, each offering different trade-offs between passband ripple and roll-off steepness.

## CHAPTER II

### METHODOLOGY

#### 1. System Design

This program implements the Pan-Tompkins algorithm for detecting QRS complexes in ECG signals. Renowned for its real-time performance and high accuracy, the algorithm processes the ECG signal through several sequential stages to enhance and isolate the QRS complexes, particularly the R-peaks. The processing pipeline is as follows:

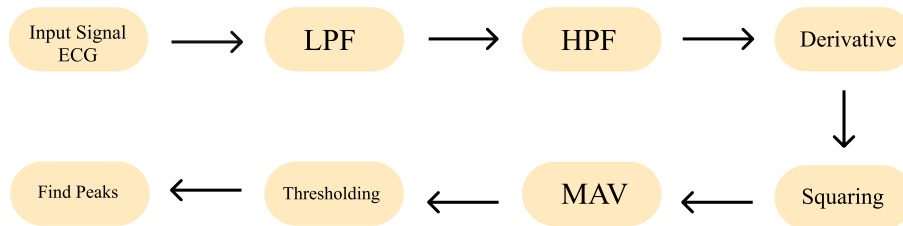


Fig 1. Block Diagram

- Input Signal: Raw ECG signal.
- Cascade Bandpass Filter: using LPF to removes high frequency noise and HPF to removes low frequency noise. These filters form a bandpass 2<sup>nd</sup> order with frequencies range from 0 – 15, which is optimal for QRS complex detection.
- Derivative: this section used to highlight the high slopes characteristic of the QRS complex.
- Squaring: from point to point, the signal is squared to make all data points positive and emphasized higher frequencies.
- MAV: moving window integrator is applied to the squared signal to obtain waveform features related to the width of the QRS complex, with window size corresponds to 150ms.
- Thresholding: It's used to be adaptive thresholding, but because a lot of error happen, and I still can't fix it until the collection time then I use the fixed threshold given by the user.
- The algorithm identifies peaks in the integrated signal that exceed the adaptive threshold and applies additional criteria to confirm the detection of R-peaks, accounting for factors like the expected refractory period and slope comparisons to avoid false detections.

#### 2. IIR Filter

A recursive (IIR) filter employs feedback: each output sample is computed from a combination of current and past input samples and one or more past output samples, which gives it its “infinite” impulse response character. In our ECG processing chain, the system is divided into three stages signal acquisition, digital filtering (IIR), and output visualization. An IIR filter's name stems from the fact that its impulse response,  $y[n]$ , never truly reaches

zero but decays indefinitely. Analog filters are naturally expressed by a Laplace-domain transfer function  $H(s)$ ; to obtain the digital counterpart  $H(z)$ , one of the most widely used techniques is the bilinear transform, which substitutes

$$s = \frac{2z - 1}{Tz + 1}$$

Fig 2. Bilinear Transform

$$y[n] = \sum_{i=0}^P b_i x[n - i] + \sum_{i=1}^Q a_i y[n - i]$$

Fig 3. Difference Equation

This this difference equation is used to implement the LPF and HPF filter in digital filter.

### 3. Tools and Software

In this project, we leveraged Visual Studio Code as the primary integrated development environment (IDE) for writing and debugging Python code, taking advantage of its rich extensions for linting, version control, and interactive notebooks. We chose NumPy chiefly as a utility library for loading ECG datasets and performing fundamental mathematical operations such as array arithmetic, vectorized computations, and statistical summaries—rather than for signal-processing routines themselves. For the user interface and rapid prototyping of our ECG-processing dashboard, I used Streamlit, which allows developers to transform ordinary Python scripts into interactive web apps with minimal boilerplate (just a few `st.*` calls) and automatic hot-reloading of code changes. Finally, Matplotlib served as our visualization engine: we used its state-machine interface to generate publication-quality plots of raw versus filtered ECG waveforms, frequency-response curves, and moving-window integration outputs, benefiting from its extensive API for figure customization and annotation.

## CHAPTER III

### RESULT AND DISCUSSION

#### 1. Filter Performance

Using arrhythmia data from the MIT database with a sampling frequency ( $f_s$ ) of 360 Hz, the filtered output shows good performance in reducing noise. The bandpass filter used eliminates noise in the range of 5 Hz to 11 Hz, which is appropriate since the ECG signal information lies within the 5 Hz to 15 Hz range. The heart rate detection results from the program are also satisfactory when the threshold is set around an amplitude of 1100. The following results were obtained from the arrhythmia data in the MIT database. In the case of the sleep apnea data, the filter also performed well in eliminating noise, using a sampling frequency of 100 Hz and a frequency range of 0.5 Hz to 15 Hz. The heart rate detection was reasonably accurate with a fixed threshold applied at an amplitude of 100.

#### 2. ECG Signal Output

The following results were obtained from the IIR digital bandpass filtering process using a cascaded mechanism of 2nd-order low-pass (LPF) and high-pass (HPF) filters.

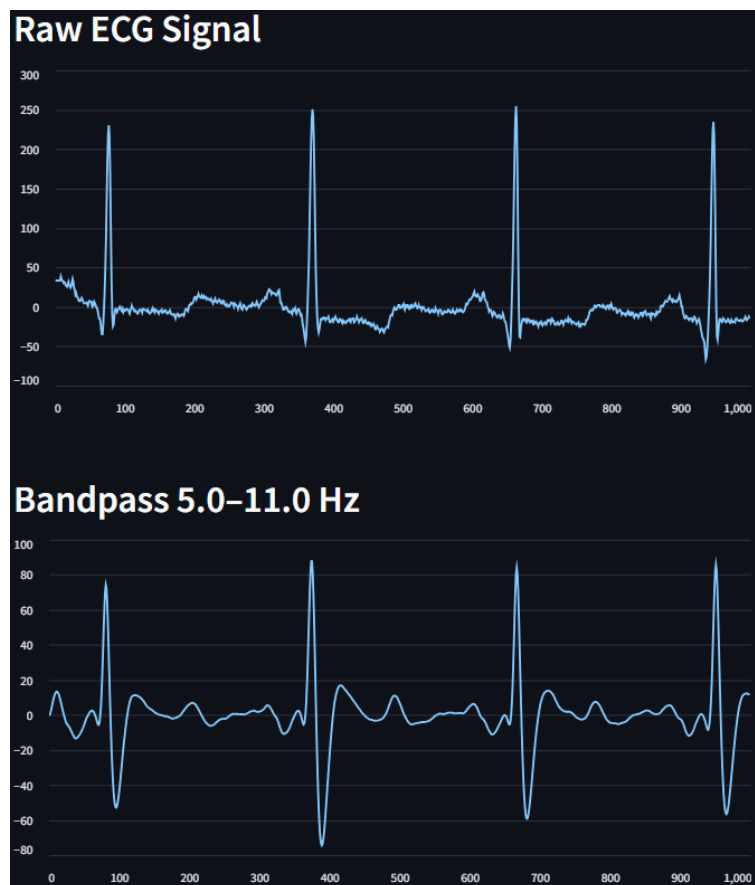


Fig 4. Bandpass Filter Results on MIT Arrhythmia Database

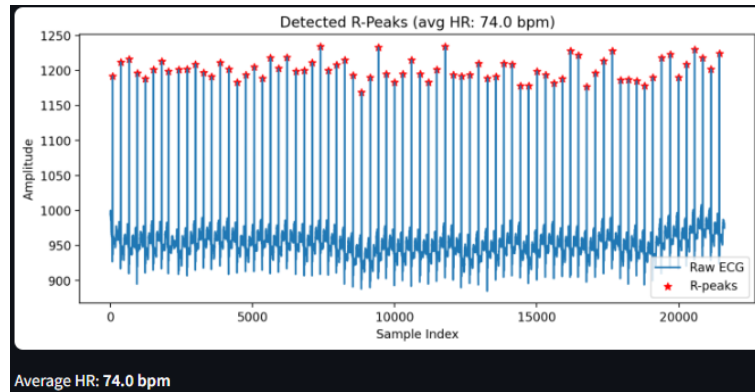


Fig 5. Heart Rate from MIT Arrhythmia Database

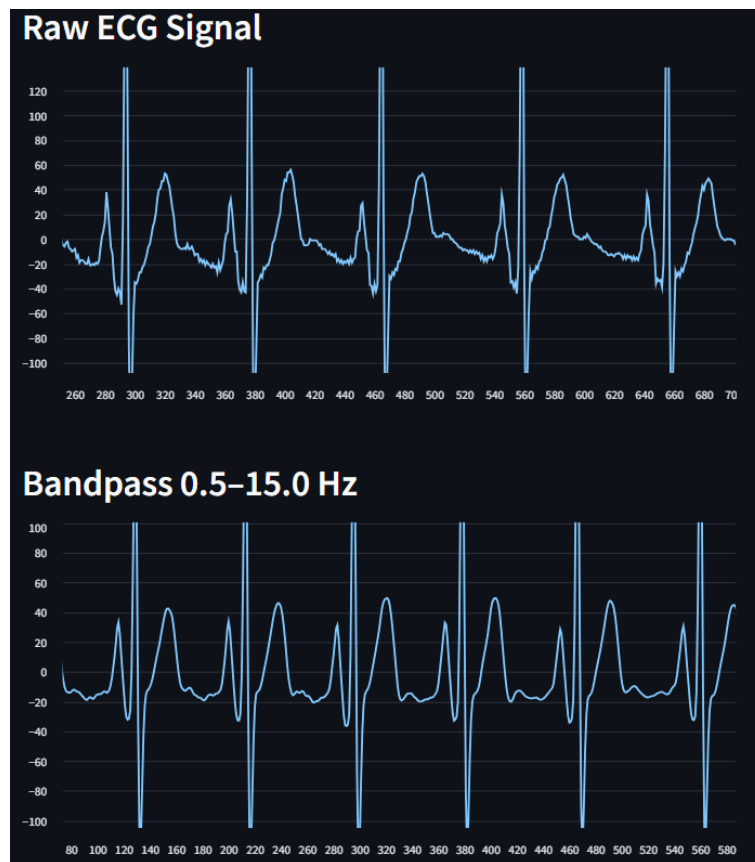


Fig 6. Bandpass Filter Results on Sleep Apnea Data

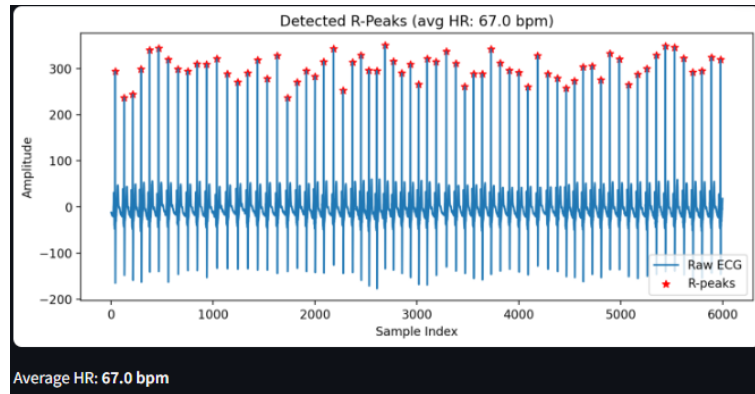


Fig 7. Heart Rate from Sleep Apnea Data

### 3. Limitations

One of the main limitations of the system is the use of a fixed threshold, which replaces the adaptive threshold typically employed in the Pan-Tompkins algorithm. The use of a fixed threshold reduces the system's responsiveness to signal variations across individuals or changes in signal quality due to external disturbances, thereby increasing the risk of detection errors, including both false positives and false negatives. Furthermore, although a bandpass filter is applied to eliminate low- and high-frequency noise, the system remains vulnerable to signal artifacts such as muscle movement noise (EMG), electrical interference, and baseline wander. The lack of further noise-handling mechanisms may reduce the accuracy of R-peak detection, especially in real-world conditions where the signal is not free from interference. Additionally, the use of a fixed-length integration window (150 ms) poses another limitation, as it does not adapt to variations in heart rate that can differ significantly between individuals.



## **CHAPTER IV**

### **CONCLUSION**

The IIR-based program utilizing a bandpass filter for QRS complex detection and heart rate calculation has not yet fully implemented the Pan-Tompkins algorithm effectively. From the perspective of the course material on digital filters, the program successfully demonstrates a well-designed digital filter by employing a cascaded system of low-pass and high-pass filters to form a bandpass filter. Moreover, the application of the bilinear transform theorem to convert the analog filter into its digital form has been carried out properly, as evidenced by the quality of the resulting filtered signal. However, the subsequent process of converting the filtered signal into heart rate data remains suboptimal due to the use of fixed threshold variables, which must be manually adjusted by the user. To improve future implementations, the program should incorporate an adaptive thresholding system that utilizes the output of the Moving Average (MAV) stage. This enhancement would allow for more accurate and robust heart rate detection across varying signal conditions.